Geological alteration of Precambrian steroids mimics early animal signatures

Lennart M van Maldegem, Benjamin J Nettersheim, Arne Leider, Jochen J Brocks, Pierre Adam, Philippe Schaeffer, Christian Hallmann

Geological alteration of Precambrian steroids mimics early animal signatures

Lennart M. van Maldegem[1,2,3#*], Benjamin J. Nettersheim[1,2#*], Arne Leider[1,2], Jochen J. Brocks[3], Pierre Adam[4], Philippe Schaeffer[4] and Christian Hallmann[1,2*]

[1] Max-Planck-Institute for Biogeochemistry, Jena, Germany
[2] MARUM – Center for Marine Environmental Sciences, University of Bremen, Bremen, Germany
[3] The Australian National University, Canberra, Australia
[4] University of Strasbourg, CNRS — UMR 7177, Strasbourg, France
[#] These authors contributed equally.
** Correspondence to lennart.vanmaldegem@anu.edu.au, benjamin.nettersheim@bgc-jena.mpg.de or challmann@bgc-jena.mpg.de*

The absence of unambiguous animal body fossils in rocks older than the late Ediacaran has rendered fossil lipids the most promising tracers of early organismic complexity. Yet much debate surrounds the various potential biological sources of putative metazoan steroids found in Precambrian rocks. Here we show that 26-methylated steranes—hydrocarbon structures currently attributed to the earliest animals—can form via geological alteration of common algal sterols, which carries important implications for paleo-ecological interpretations and inhibits the use of such unconventional 'sponge' steranes for reconstructing early animal evolution.

Determining the first appearance of animals in the rock record places important constraints on the timing and environmental conditions surrounding the Neoproterozoic advent of organismic complexity. In particular the perceived late rise of animals—nearly a billion years after the first fossil eukaryotic cells emerge in the rock record ~1600 million years ago[1,2] (Ma)—remains one of the fundamental unexplained phenomena of evolution. Resolving the drivers for the emergence of organismic complexity fundamentally relies on a reliable temporal framework of animal evolution. In this regard, occurrences of Cambrian sponge spicules[3–5] and animal fossils of unspecific affinity (~560 Ma[6]) are preceded by a much earlier record (up to ~640 Ma[7–9]) of unconventional fossil steroid lipids (i.e. steranes) considered diagnostic for early sponges and thus for animal-grade life. Timing the rise of complex life thus crucially depends on the applicability of these biomarker hydrocarbons, which warrants thorough scrutinisation.

In contrast to the ubiquitous C_{27} steroid biomarker cholestane, which derives from cholesterol (C_{27})—the major membrane sterol in most animals—peculiar C_{30} sponge sterane biomarkers carry an additional *n*-propyl (24-npc) or isopropyl (24-ipc) alkyl group at position C-24, or an ethyl group at C-24 combined with an additional methyl group at position C-26 at the end of the steroid side-chain (26-mes) (Figs. 1, 2). In the geological record, 24-ipc and 26-mes are particularly abundant in upper Neoproterozoic rocks, preceding animal fossils by almost 100 Myr[7,8] (Fig. 1). Other unconventional steranes with C-26 alkylation are found in even older deposits: 26-methylcholestane (26-mec, or cryostane) and tentatively identified 26-propylcholestane (26-proc) have been reported in rocks antedating the Cryogenian Snowball Earth glaciations (717–635 Ma)[9–12] (Fig. 1). The biological capacity to alkylate the steroid side-chain at position C-26 is indeed very

rare, yet present in many demosponges[8] and the various 26-alkylsteroids were proposed to extend the metazoan biomarker record into the Cryogenian Period and possibly even into the Tonian (717–1000 Ma)[8,9]. However, the sponge interpretation of some of these fossil lipids has been challenged[13–17]. Ecological arguments and the presence of 24-ipc and 26-mes in lipid hydrogenates of planktonic, unicellular Rhizaria—the protist group including Foraminifera and Radiolaria—have cast doubt on whether these C_{30} steranes are sufficiently diagnostic for animals[16,17]. Still, other scientists maintain that, from a perspective of abundances, only demosponges can account for the biomarker patterns typically observed in Neoproterozoic-Cambrian rocks[18]. Precursors to the 26-alkylsteranes 26-mec and 26-proc are not known to be biosynthesised by protists or any other organism. Hence a confirmed unique sponge source[9] would greatly impact our understanding of early animal evolution.

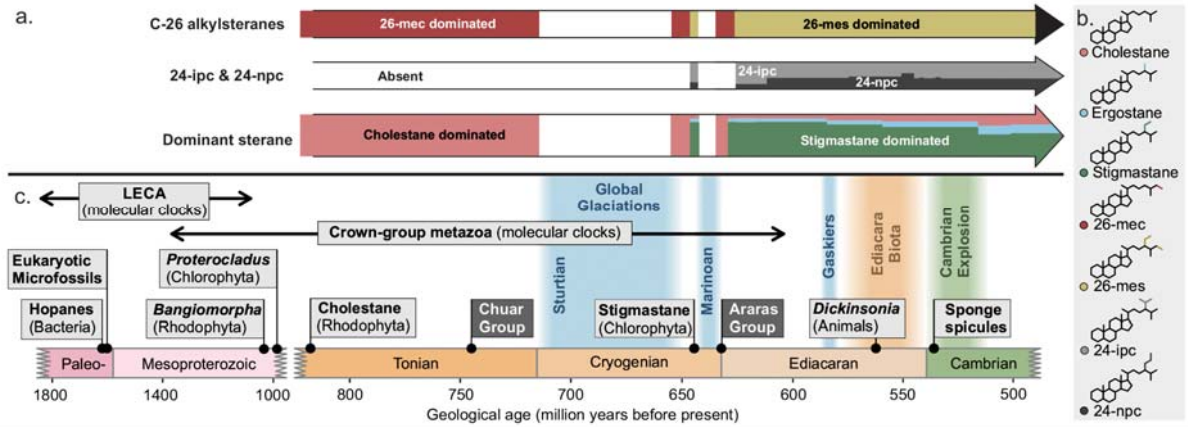

Figure 1. Geological record of steroid evolution. (a.) Arrows indicate the presence of 26-methylcholestane (26-mec)[12] and 26-methylstigmastane (26-mes)[8], the relative distribution of 24-isopropylcholestane (24-ipc) and 24-*n*-propylcholestane (24-npc)[7,8], and the distribution of conventional (C_{27}, C_{28} and C_{29}) steranes[10,26] throughout the Neoproterozoic and earliest Phanerozoic. **(b.)** Molecular structures of relevant steranes. **(c.)** Key events in Proterozoic Earth system evolution. Black arrows mark the emergence of the last eukaryotic common ancestor (LECA) and evolution of crown-group metazoa, as suggested by molecular clocks[36,37]; light grey tags in the Paleo- and Mesoproterozoic indicate the oldest known evidence for bacterial hopane biomarkers[38], unambiguous eukaryotic microfossils[1] and multicellular algal fossils[27,39]. The earliest animals occur among the Ediacara biota[6], whilst the oldest sponge spicules are observed in the lower Cambrian[3–5]. Dark grey tags mark the depositional ages of the sedimentary sequences used in this study.

Based on new biomarker analyses, we find that sedimentary rocks of the ~740 Ma Chuar Group and the 635 Ma Araras Group contain not only 26-mec and 26-proc, which could represent sponge markers[8,9], but a complete homologous series of 26-alkylcholestanes with side-chain alkylation extending from C_1 to at least C_8. The abundance of consecutive homologs exhibits an exponential decrease (Fig. 2a, b), which is uncommon for a series of biosynthetic products but reminiscent of patterns created by abiogenic processes such as free-radical alkyl additions[19] or the thermal cracking of longer alkane moieties (*Supplementary Information*). In all observed cases, the 26-alkylsterane series co-occur with extended series of 3-alkylsteranes that exhibit remarkably similar homolog patterns (Fig. 2a–c), suggesting a common mechanistic origin. Such 3-alkylsterane series have been previously reported and were attributed to diagenetic reactions, possibly proceeding *via* the bacterial modification of sedimentary

ster-2-ene intermediates[20,21]. Our observation of a nearly identical alkylation pattern in 3- and 26-alkylsteranes thus also suggests a diagenetic origin of 26-alkylation.

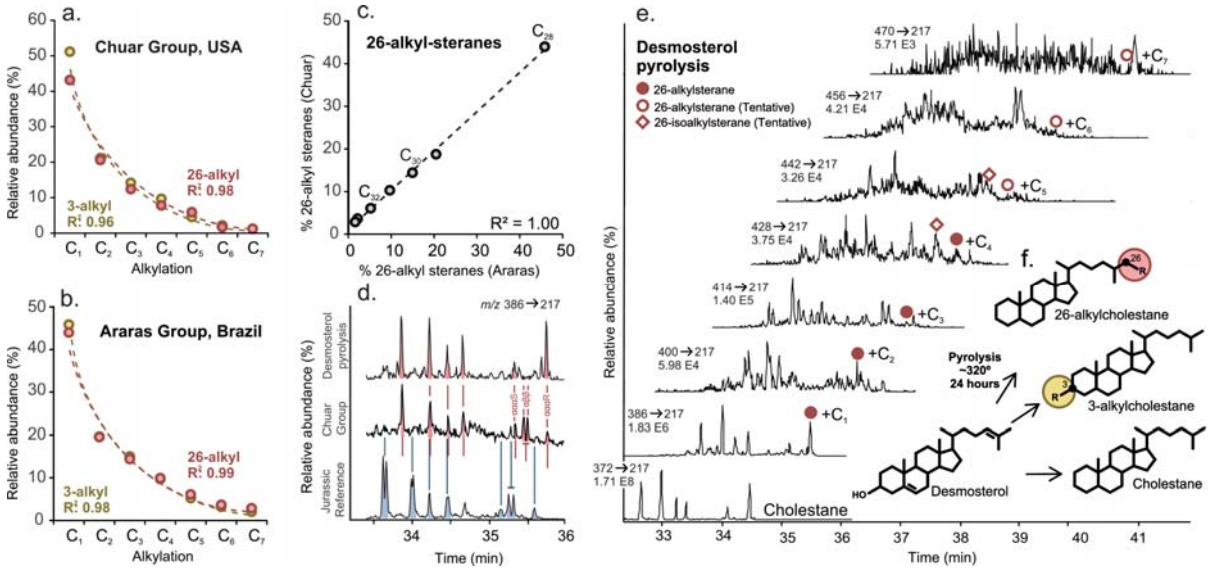

Figure 2. Alkylsteranes in Neoproterozoic rocks and in sterol pyrolysates. Cross plots show the relative distribution of 3- and 26-alkylcholestanes in (**a.**) the ~740 Ma Chuar Group (#L.39)[40], and (**b.**) the 635 Ma Araras Group (#TeS-22)[40]; see Supplementary Information for sample pedigrees).(**c.**) The relative distribution pattern of 26-alkylsteranes in the Chuar Group matches that in the ~100 Myr younger Araras Group. (**d.**) C_{28} sterane (*m/z* 386→217) GC-MS traces show the presence of 26-methylcholestanes (red peaks) in a laboratory pyrolysate (desmosterol, 300ºC, #8 in Supplementary Table 1) and in a Neoproterozoic rock extract (Chuar Group; #L.38), which differ from ergostanes (i.e. 24-methylcholestanes; blue peaks) commonly present in Phanerozoic rocks and oils (here shown in Phanerozoic oil standard NSO-1); also see Supplementary Figure 1. (**e.**) Pyrolysis of desmosterol creates a series of 26-alkylsteranes. Closed circles mark C_1–C_4 alkylcholestane peaks in same elution position as ααR isomers in Neoproterozoic rock extracts (the identity of the ααR isomer of 26-mec cholestane was additionally confirmed through coelution experiments with an authentic standard); open circles mark consecutive peaks of the same homologous series tentatively assigned as C_5–C_8 alkylcholestanes; also see Supplementary Information. (**f.**) Molecular structures and reaction schematic of precursor (desmosterol) alkylation or reduction (colours match those

To determine if alkylation can indeed occur through typical diagenetic reactions, and to assess similarities between 3- and 26-alkylsterane formation, we conducted closed-vessel pyrolysis experiments of pure sterols in glass tubes alongside graphite or active charcoal and heated the material to 300º, 310º or 340ºC for 24 hours (see *Supplementary Information* for details). This common method is a laboratory analogue for organic matter alteration during burial[22], where the solid carbon phases act as catalysts[23,24] and facilitate hydrogen and carbon transfer reactions[25] (*Supplementary Information*). The highest relative abundances of 26-mec occur in Tonian–Cryogenian rocks that otherwise exhibit a strong dominance of cholestanes[10,26] (Fig 1). Apart from animals, such high C_{27} steroid abundances are the hallmark of red algae[10], the fossil record of which extends to at least 1.1 Ga[27] (Fig. 1). In addition to cholesterol, many rhodophytes tend to biosynthesise abundant side-chain functionalised C_{27} steroids, such as desmosterol or 25-hydroxylated cholesterols[28,29], rendering these compounds likely diagnostic indicators of Tonian primary producers. In all our experiments with educts containing a hydroxyl functionality at C-3 (cholesterol, 5-dihydrocholesterol [cholestanol], 24-dehydrocholesterol [desmosterol] and 25-hydroxycholesterol), pyrolysis products comprised a series of C-3

alkylated steranes extending at least to C_8—similar to alkylation patterns in Neoproterozoic rock extracts. In contrast, only educts with a less common side-chain functionalisation (desmosterol, 25-hydroxycholesterol) yielded a similar series of 26-alkylsteranes (Fig. 2d–f; Supplementary Figure 1), suggesting that biological functionalisation is required for geological alkylation. The latter may proceed *via* radical-chain reactions that are known to induce alkylation of alkenes and alcohols at low temperatures[19] and which may operate during early diagenesis and even in the water column[30], and/or by ionic reactions that are well known to occur in sedimentary rocks[31] (*Supplementary Information*). In our pyrolysis experiments, the thermochemical alteration of regular desmethylsterols on solid carbon surfaces generated relevant yields of 3-methylcholestane and 26-methylcholestane (up to 2.5% and 2.0% relative to cholestane, respectively; *Supplementary Table* 1), comparable to abundances of 26-methylcholestanes in Neoproterozoic rocks (2–8%, see Zumberge et al. 2019 and *Supplementary Table* 2). Bacterially-mediated rearrangement processes[32] thus do not need to be invoked. Purely abiotic geological processes can create unconventional 'sponge' steranes from regular (*i.e.* algal) sterol precursors in significant yields, thereby negating any animal[7,8,18,33] or protozoan[16,17] diagnosticity.

The putative sponge-derived C_{30} sterane 26-mes is found in Neoproterozoic and Cambrian (n > 60), and in Phanerozoic (n = 8) rocks and oils that are dominated by C_{29} steranes[8], whereas the C_{28} alkylsterane 26-mec is found in rocks that are dominated by C_{27} steranes[12,26] (n > 11[9]; see Fig. 1). This carbon number relationship (n+1 *vs.* n) likely indicates a mechanistic connectivity[8]. But rather than pointing to the heterotrophic transformation of dietary sterols by sponges[8], we attribute Neoproterozoic 26-mec and 26-mes to the abiogenic diagenetic modification of sedimentary C_{27} and C_{29} sterols, respectively. Pyrolysis experiments with various side-chain unsaturated C_{29} phytosterols (*i.e.* $\Delta^{5,22}$-stigmastadienol [stigmasterol], $\Delta^{5,24(28)}$-stigmastadienol [fucosterol] and $\Delta^{5,25}$-stigmastadienol [clerosterol]) indeed confirm that also the supposedly sponge-diagnostic C_{30} sterane marker 26-mes[8] can form from regular C_{29} sterol precursors. Abundances of 26-mes in pyrolysates of up to 0.8% relative to stigmastane are comparable to those encountered in Neoproterozoic-Cambrian samples (0.3–4.2%, average 1.5%, n = 61, calculated from Zumberge et al. 2018[8], see *Supplementary Information*), demonstrating that diagenetic alteration of C_{29} sterol precursors can realistically account for 26-mes abundances in the rock record.

In summary, none of the low-concentrated 26-alkylated sponge associated steranes found in the ancient rock record (26-mec, 26-proc and 26-mes) are diagnostic for early Metazoa or for Rhizaria, nor are any of the other possible sponge biomarkers (24-ipc, 24-npc), as shown by independent work in this issue[34]. Therefore, the Neoproterozoic steroid record should not be used as a minimum estimate for timing the origin of the characteristic sponge body plan or the emergence of animal multicellularity, as previously suggested[9]. The observation that diagenetic reactions of common algal sterols may create all of the currently-used sponge biomarkers in sufficient abundances to account for geological observations re-accentuates the importance of ~560 Ma Ediacara Biota fossils[6,35] (Fig. 1) and Cambrian sponge fossils and spicules[3–5] (Fig. 1) as the oldest evidence for animals and sponges, respectively. The assumption that characteristic hydrocarbon alkylation

patterns define the biological diagnosticity and affinity of particular fossil lipids forms a fundamental pillar of the biomarker concept. Our finding that non-biological processes can mimic seemingly diagnostic alkylation patterns in steranes—and presumably in many other biomarkers—implies that the correct interpretation of the ancient biomarker record will require more insight into reliably recognising such diagenetic signals. Nevertheless, the discovery of functionalisation-dependent alkylation carries vast paleobiological potential by providing new perspectives to reconstruct past biodiversity and the evolution of lipid biosynthetic pathways.

Methods

Rock samples

Rock samples from the Tonian Chuar Group (USA) and earliest Ediacaran Araras Group (Brazil) were analysed as reported previously[40–42]. Chuar Group samples were collected on the northwest flank of Nankoweap Butte (36º26'43" N, 111º88'40" W), while samples of the Araras Group were collected from Terconi quarry (15º40'42" S, 58º4'32" W). The particular Chuar sample shown in Figure 2 and Supplementary Figures 1 and 2 derives from the Walcott Member (sample #L.38 in Van Maldegem, 2017[42], and #L.39 in Van Maldegem et al., 2019[40]), at a stratigraphic height 287.6 m above the boundary to the Galeros Fm. The particular Araras sample shown in Figure 2 derives from the Mirassol d'Oeste Fm. (sample #TeS-22 in Van Maldegem, 2017[40], and Van Maldegem et al., 2019[42]), at a stratigraphic height 11.5 m above the base of the cap carbonate. In short, rocks were cleanly sawed into interior and exterior subsamples for syngeneity assessment as previously reported[42], extracted using dichloromethane (DCM), fractionated into aliphatic (sats), aromatic and polar fractions using small-scale open column liquid chromatography using activated silica and analysed by GC-MS. The presence of 26-mec and 26-proc in Chuar Group extracts has been reported previously[9,10,12,43] while extended series of 3-alkylcholestanes have previously been reported for Araras Group extracts[44].

Pyrolysis experiments

To simulate the geological processes that affect biological sterols upon sediment burial, we subjected functionalised sterols to thermal maturation experiments in the presence of two different carbon phases[cf.22]: graphite (C, TIMREX KS75 primary synthetic graphite, microcrystalline, TIMCAL Ltd.) and activated carbon (Sigma-Aldrich, DARCO, 100 mesh particle size, CAS: 7440-44-0). The following sterols were used in this study: 5,24(28)-stigmastadienol (fucosterol; ≥ 98%, Cayman Chemical Company), 5,25-stigmastadienol (clerosterol; ≥ 98%, ChemFaces), stigmasterol (≥ 95%, Santa Cruz Biotechnology), 5α(H)-cholestanol (≥ 95%, Sigma-Aldrich), cholesterol (≥ 99%, Sigma-Aldrich), 25-hydroxycholesterol (≥ 98%, Sigma-Aldrich), 5α(H)-cholest-2-ene (R205982, Sigma-Aldrich), and 5,24-cholestadienol (desmosterol; ≥ 98%, Cayman Chemical Company). In most experiments, between ~1 and 6 mg solid carbon and ~0.5 and 1 mg sterol were used. Laboratory metal- and glassware was baked at 500ºC for 8 h to remove potential hydrocarbon contamination. Graphite and activated carbon were activated by heating (> 12 h at 110ºC) and subsequently stored at 110ºC, but may have re-adsorbed

variable small amounts of atmospheric moisture before the tubes were sealed. Sterols and solid carbon phases were transferred into glass tubes flame sealed at one end (Duran, 8 mm diameter, 1 mm wall thickness) with a spatula and/or dissolved in organic solvent. Upon solvent evaporation, tubes were evacuated to ≤ 300 mTorr and flame sealed with a gas torch. To test if active glass surfaces of the reaction vessel could have influenced the experimental alkylation reactions, glass tubes were deactivated with dichlorodimethylsilane (5% in toluene[cf.22]) in some experiments (see Supplementary Table 1). Selected experiments saw the addition of *n*-alkanes (*n*-hexane or *n*-pentadecane; originally ~20 µL, but only a fraction of *n*-hexane remained after evacuation of the tube) in addition to the steroids to test the effect on alkylation yields. Supplementary Tables 1 and 4 give an overview of the different experimental conditions. After pyrolysis, tubes were cooled to room temperature and the solid carbon phase content was transferred with sequential rinses of *n*-hexane, DCM and methanol (MeOH) onto silica gel in either a Pasteur-pipette or in a 4 mL SPE glass tube, and subsequently extracted with ~10 mL *n*-hexane, ~10 mL DCM and ~4 mL MeOH (experiments #2, #3 and #20 were extracted with ~3 mL DCM and ~10 mL *n*-hexane only). Once solvents were evaporated under a gentle stream of N_2, the solvent extracts were re-dissolved in *n*-hexane for GC-MS analyses. In most cases, aliphatic fractions (obtained by eluting ~1.5 dead volume *n*-hexane over a Pasteur-pipette filled with activated silica gel) were used for GC-MS-based quantifications in multiple reaction monitoring (MRM) mode. Empty sealed glass tubes taken through the same process were used as procedural blanks.

GC-MS analyses and biomarker identification

Biomarker analyses were conducted on a Thermo Quantum XLS Ultra triple quadrupole MS coupled to a Thermo Trace GC Ultra. Details of the analyses of Chuar and Araras Group extracts have been previously reported[40]. For the analysis of hydrocarbons from pyrolysates, the GC was fitted with a VF-1 MS column (40 m, 0.15 mm i.d., 0.15 µm film thickness). A constant flow of Helium (5.0, Westfalen AG) was used as carrier gas (1.0 mL/min). Volumes of 1 out of 20–2000 µL were injected at 40ºC in splitless mode (held for 0.1 min) using a Thermo 816 RP-2004 PTV injector and ramped to 330ºC at 14.5ºC/sec (held for 2.0 min). The oven was held isothermal at 40ºC (2.5 min), then heated to 325ºC at 8ºC/min and held at the final temperature for 22 min. Ionisation was achieved by electron impact at 70 eV with an emission current of 50 or 100 µA and at a source temperature of 250ºC. Q1 and Q3 were each operated in 0.7 Da resolution with a cycle time of 0.5 s. Q2 was operated with Argon 6.0 collision gas at a pressure of 1.0 mTorr and a collision voltage of 10 eV. Steranes were analysed and quantified in MRM mode monitoring M^+ to base ion (*m/z* 217 for desmethyl and 26-alkylsteranes, *m/z* 231 for 2- and 3-methylsteranes) transitions. For analyses of extended 3-alkylsterane series, higher homologs of the 3-alkylcholestane series were analysed with $M^+ \rightarrow$ (217+x*14) transitions (x representing the number of carbon atoms attached to C-3).

Steranes were identified in comparison to published elution patterns[e.g.21,45] as well as by parallel analyses of the Norwegian standard oil mixture NSO-1[46], extracts from the Araras formation (as various 3-alkylcholestanes were identified in Araras Group extracts through coelution experiments with synthetic standards[44]) and additional Neoproterozoic-Cambrian bitumens, such as extracts from the Usolye Formation[cf.26]. For pyrolysates, the

identity of the 5α(H),14α(H),17α(H) (20*R)* (abbreviated ααα*R*) isomers of 26-mes, 26-mec, 3-ethylcholestane, 3-*n*-propylcholestane and 3-methylstigmastane was further confirmed by GC-MS co-injection experiments with rock extracts, a 26-mes-containing *Rhabdastrella distincta (R. distincta)* demosponge Hydrous Pyrolysis (HyPy) extract[8] kindly provided by Gordon Love (University of California Riverside), and authentic 3-ethylcholestane[47], 3-*n*-propylcholestane, 3-methylstigmastane[47] and 26-methylcholestane[43] standards that were synthesised at the University of Strasbourg.

References

1. Lamb, D. M., Awramik, S. M., Chapman, D. J. & Zhu, S. Evidence for eukaryotic diversification in the ~1800 million-year-old Changzhougou Formation, North China. *Precambrian Res.* **173**, 93–104 (2009).
2. Knoll, A. H. & Nowak, M. A. The timetable of evolution. *Sci. Adv.* **3**, 1–14 (2017).
3. Antcliffe, J. B., Callow, R. H. T. & Brasier, M. D. Giving the early fossil record of sponges a squeeze. *Biol. Rev.* **89**, 972–1004 (2014).
4. Chang, S., Zhang, L., Clausen, S., Bottjer, D. J. & Feng, Q. The Ediacaran-Cambrian rise of siliceous sponges and development of modern oceanic ecosystems. *Precambrian Res.* **333**, 105438 (2019).
5. Xiao, S., Hu, J., Yuan, X., Parsley, R. L. & Cao, R. Articulated sponges from the Lower Cambrian Hetang Formation in southern Anhui , South China : their age and implications for the early evolution of sponges. *Palaeogeogr. Palaeoclimatol. Palaeoecol.* **220**, 89–117 (2005).
6. Bobrovskiy, I. *et al.* Ancient steroids establish the Ediacaran fossil Dickinsonia as one of the earliest animals. *Science* **361**, 1246–1249 (2018).
7. Love, G. D. *et al.* Fossil steroids record the appearance of Demospongiae during the Cryogenian period. *Nature* **457**, 718–721 (2009).
8. Zumberge, J. A. *et al.* Demosponge steroid biomarker 26-methylstigmastane provides evidence for Neoproterozoic animals. *Nat. Ecol. Evol.* **2**, 1709–1714 (2018).
9. Zumberge, J. A., Rocher, D. & Love, G. D. Free and kerogen-bound biomarkers from late Tonian sedimentary rocks record abundant eukaryotes in mid-Neoproterozoic marine communities. *Geobiology* **18**, 326–347 (2020).
10. Brocks, J. J. *et al.* The rise of algae in Cryogenian oceans and the emergence of animals. *Nature* **548**, 578–581 (2017).
11. Brocks, J. J. The transition from a cyanobacterial to algal world and the emergence of animals. *Emerg. Top. Life Sci.* 1–10 (2018).
12. Brocks, J. J. *et al.* Early sponges and toxic protists: Possible sources of cryostane, an age diagnostic biomarker antedating Sturtian Snowball Earth. *Geobiology* **14**, 129–149 (2016).
13. Antcliffe, J. B. The oldest compelling evidence for sponges is still early Cambrian in age - Reply to Love and Summons (2015). *Palaeontology* **58**, 1137–1139 (2015).
14. Botting, J. P. & Muir, L. A. Early sponge evolution: A review and phylogenetic framework. *Palaeoworld* **27**, 1–29 (2018).
15. Botting, J. P. & Nettersheim, B. J. Searching for sponge origins. *Nat. Ecol. Evol.* **2**, 1685–1686 (2018).
16. Nettersheim, B. J. *et al.* Putative sponge biomarkers in unicellular Rhizaria question an early rise of animals. *Nat. Ecol. Evol.* **3**, 577–581 (2019).
17. Hallmann, C. *et al.* Reply to: Sources of C_{30} steroid biomarkers in Neoproterozoic – Cambrian rocks and oils. *Nat. Ecol. Evol.* **4**, 37–39 (2020).
18. Love, G. D. *et al.* Sources of C_{30} steroid biomarkers in Neoproterozoic – Cambrian rocks and oils. *Nat. Ecol. Evol.* **4**, 34–46 (2020).
19. Urry, W. H., Stacey, F. W., Huyser, E. S. & Juveland, O. O. The Peroxide- and Light-induced Additions of Alcohols to Olefins. *J. Am. Chem. Soc.* **76**, 450–455 (1954).
20. Summons, R. E. & Capon, R. J. Identification and significance of 3β-ethyl steranes in sediments and petroleum. *Geochim. Cosmochim. Acta* **55**, 2391–2395 (1991).
21. Summons, R. E. & Capon, R. J. Fossil steranes with unprecedented methylation in ring-A. *Geochim. Cosmochim. Acta* **52**, 2733–2736 (1988).
22. Alexander, R., Berwick, L. & Pierce, K. Single carbon surface reactions of 1-octadecene and 2,3,6-trimethylphenol on activated carbon: Implications for methane formation in sediments. *Org. Geochem.* **42**, 540–547 (2011).
23. Given, P. H. & Hill, L. W. Catalysis of the isomerisation and polymerisation of olefins on carbon blacks. *Carbon* **6**, 525–535 (1968).

24. Meier, J. A. & Hill, L. W. Carbon black catalyzed olefin isomerization: A heterogeneous site model based on rate dependence on catalyst concentration. *J. Catal.* **87**, 80–87 (1974).
25. Alexander, R., Dawson, D., Pierce, K. & Murray, A. Carbon catalysed hydrogen exchange in petroleum source rocks. *Org. Geochem.* **40**, 951–955 (2009).
26. Hoshino, Y. *et al.* Cryogenian evolution of stigmasterol biosysnthesis. *Sci. Adv.* **3**, 1–7 (2017).
27. Butterfield, N. J., Knoll, A. H. & Swett, K. A bangiophyte red alga from the proterozoic of arctic Canada. *Science* **250**, 104–107 (1990).
28. Idler, D. R., Saito, A. & Wiseman, P. Sterols in red algae (Rhodophyceae). *Steroids* **11**, 465–473 (1968).
29. Fattorusso, E. *et al.* Sterols of some red algae. *Phytochemistry* **14**, 1579–1582 (1975).
30. Adam, P., Philippe, E. & Albrecht, P. Photochemical sulfurization of sedimentary organic matter: A widespread process occurring at early diagenesis in natural environments? *Geochim. Cosmochim. Acta* **62**, 265–271 (1998).
31. Rubinstein, B. I., Sieskind, O. & Albrecht, P. Rearranged sterenes in a shale: Occurrence and simulated formation. *Org. Geochem.* **11**, 1973–1976 (1975).
32. Dahl, J. E., Moldowan, J. M., McCaffrey, M. A. & Lipton, P. A. A new class of natural products revealed by 3β-alkyl steranes in petroleum. *Nature* **355**, 472–475 (1992).
33. McCaffrey, M. A. *et al.* Paleoenvironmental implications of novel C_{30} steranes in Precambrian to Cenozoic Age petroleum and bitumen. *Geochim. Cosmochim. Acta* **58**, 529–532 (1994).
34. Bobrovskiy, I. *et al.* Algal origin of sponge sterane biomarkers negates the oldest evidence for animals in the rock record. *Nat. Ecol. Evol.* This Issue
35. Xiao, S. & Laflamme, M. On the eve of animal radiation: Phylogeny, ecology and evolution of the Ediacara biota. *Trends Ecol. Evol.* **24**, 31–40 (2008).
36. Parfrey, L. W., Lahr, D. J. G., Knoll, A. H. & Katz, L. A. Estimating the timing of early eukaryotic diversification with multigene molecular clocks. *Proc. Natl. Acad. Sci. U. S. A.* **108**, 13624–13629 (2011).
37. Erwin, D. H. *et al.* The Cambrian Conundrum: Early Divergence and Later Ecological Success in the Early History of Animals. *Science* **334**, 1091–1097 (2011).
38. Brocks, J. J. *et al.* Biomarker evidence for green and purple sulphur bacteria in a stratified Palaeoproterozoic sea. *Nature* **437**, 866–870 (2005).
39. Tang, Q., Pang, K., Yuan, X. & Xiao, S. A one-billion-year-old multicellular chlorophyte. *Nat. Ecol. Evol.* **4**, 543-549 (2020).
40. van Maldegem, L. M. *et al.* Bisnorgammacerane traces predatory pressure and the persistent rise of algal ecosystems after Snowball Earth. *Nat. Commun.* **10**, 1–11 (2019).
41. Hallmann, C., Kelly, A. E., Gupta, S. N. & Summons, R. E. Reconstructing deep-time biology with molecular fossils. in *Quantifying the Evolution of Early Life* 355–401 (Springer Netherlands, 2011).
42. van Maldegem, L. M. *Molecular and isotopic signatures of life surrounding the Neoproterozoic Snowball Earth events*. *PhD Dissertation, University of Bremen* (https://media.suub.uni-bremen.de/handle/elib/1535, 2017).
43. Adam, P., Schaeffer, P. & Brocks, J. J. Synthesis of 26-methyl cholestane and identification of cryostanes in mid-Neoproterozoic sediments. *Org. Geochem.* **115**, 246–249 (2018).
44. Sousa Júnior, G. R. *et al.* Organic matter in the Neoproterozoic cap carbonate from the Amazonian Craton, Brazil. *J. South Am. Earth Sci.* **72**, 7–24 (2016).
45. Dahl, J. E. *et al.* Extended 3β-alkyl steranes and 3-alkyl triaromatic steroids in crude oils and rock extracts. *Geochim. Cosmochim. Acta* **59**, 3717–3729 (1995).
46. Weiss, H. The Norwegian industry guide to organic geochemical analyses. *Ed. 4.0 Nor. Hydro Statoil, Geolab Nor. SINTEF Pet. Res. Nor. Pet. Dir.* (2006).
47. Schaeffer, P., Fache-Dany, F., Trendel, J. M. & Albrecht, P. Polar constituents of organic matter rich marls from evaporitic series of the Mulhouse basin. *Org. Geochem.* **20**, 1227–1236 (1993).

Acknowledgements

We thank Rafael Tarozo and Paul Pringle for laboratory support, Ilya Bobrovskiy for discussions and helpful comments on the manuscript, Pierre Sansjofre for sharing Araras Group samples, the National Park Service (GRCA-00645) for permission to sample the Chuar Group, and Gordon Love for providing a 26-mes reference sample. This work was funded by the Max-Planck-Society and the Deutsche Forschungsgemeinschaft (Research Center/Cluster of Excellence 309: MARUM - Center for Marine Environmental Sciences). We further acknowledge the French

National Research Agency (CNRS; P.S. and P.A.) and Australian Research Council (grant nos. DP1095247 and DP160100607 to J.J.B.).

Author Contributions

L.M.v.M., B.J.N., and C.H. designed the research, analysed all geochemical data and wrote the manuscript with input from A.L., J.J.B., P.S. and P.A. who also assisted with interpretation. L.M.v.M. conducted the geological analyses. B.J.N. and A.L. performed pyrolysis experiments on modern sterols. P.A. and P.S. synthesised standards of 3-alkylsteranes and 26-methylcholestane.

Competing Interests statement

The authors declare no competing interests.

Data Availability Statement

All data is available in the Supplementary Information

Supplementary Information for

Geological alteration of Precambrian steroids mimics early animal signatures

Lennart M. van Maldegem[1,2,3#]*, Benjamin J. Nettersheim[1,2#]*, Arne Leider[1,2], Jochen J. Brocks[3], Pierre Adam[4], Philippe Schaeffer[4] and Christian Hallmann[1,2]*

[1] Max-Planck-Institute for Biogeochemistry, Jena, Germany
[2] MARUM – Center for Marine Environmental Sciences, University of Bremen, Germany
[3] The Australian National University, Canberra, Australia
[4] University of Strasbourg, CNRS — UMR 7177, Strasbourg, France
[#] These authors contributed equally
**Correspondence to lennart.vanmaldegem@anu.edu.au, benjamin.nettersheim@bgc-jena.mpg.de or challmann@bgc-jena.mpg.de*

This PDF file includes:

1) Pyrolytic formation of C_{28} alkylsteranes from C_{27} sterols

The *m/z* 386→217 chromatograms of rock extracts of most Tonian (1000–720 Ma) biomarker-bearing samples (e.g. from the ~729–757 Ma Chuar Group[1] in the USA and the ~886–740 Ma Visingsö Group in Sweden[2], as well as the terminal Cryogenian ~635 Ma Araras Group in Brazil[3]) are characterised by a series of 26-methylcholestane (26-mec, or 'cryostane') peaks (Supplementary Figures 1c, 2c). The 26-methylated cholestanes elute significantly later than the corresponding 24-methylated cholestane isomers (ergostanes), which are present in most Phanerozoic oils and sedimentary rock extracts (Supplementary Figure 1e). In Chuar Group extracts, the 26-mec series comprises four diasterane (re-arranged steranes that occur in the majority of oils and bitumens as exemplified for ergostanes in the Phanerozoic North Sea NSO-1 oil standard in Supplementary Figure 1e) and four regular sterane peaks. This pattern is closely mirrored by extracts of laboratory desmosterol thermal maturation experiments employing active carbon (Supplementary Figures 1b, 2d) or graphite (Supplementary Figure 1d) as reactive surfaces. The four main diasterane isomers as well as the regular ααα*R* 26-mec isomer all formed during carbon-based pyrolysis. Under the mild pyrolytical conditions, which we specifically chose to mimic diagenetic and early catagenetic reactions, only the thermally less stable ααα*R* isomer formed amongst regular steranes (i.e. no epimerisation at C-14, C-17 and C-20 occurred[cf.4]). In contrast to our short-term laboratory heating experiments, during long-term maturation associated with geological burial (or during pyrolysis experiments employing longer duration or higher temperatures), the thermally less stable ααα*R* isomer can be expected to be transformed into an equilibration mixture containing all four regular isomers[4], as observed in the Neoproterozoic sediments. Our pyrolysis experiments thus suggest that Tonian C_{28} sterane signatures may form via sedimentary alteration of side-chain functionalised C_{27} sterols.

As exemplified for desmosterol in Supplementary Figure 2, the pyrolysate signatures of side-chain functionalised sterols not only closely match that of Chuar Group extracts in *m/z* 386→217 (i.e. C_{28} side-chain methylated steranes), but also in *m/z* 386→231 (i.e. C_{28} A-ring methylated steranes) and *m/z* 372→217 chromatograms (i.e. C_{27} desmethylsteranes). This similarity suggests that the geological alteration of regular C_{27} steroids may explain many steroidal characteristics of Tonian rock extracts without the requirement for specific biological source input. Even the relative abundances of cholestanes, 26-methylcholestanes, the different A-ring methylated cholestanes and the regular *versus* diasterane abundances are remarkably similar (Supplementary Figure 2).

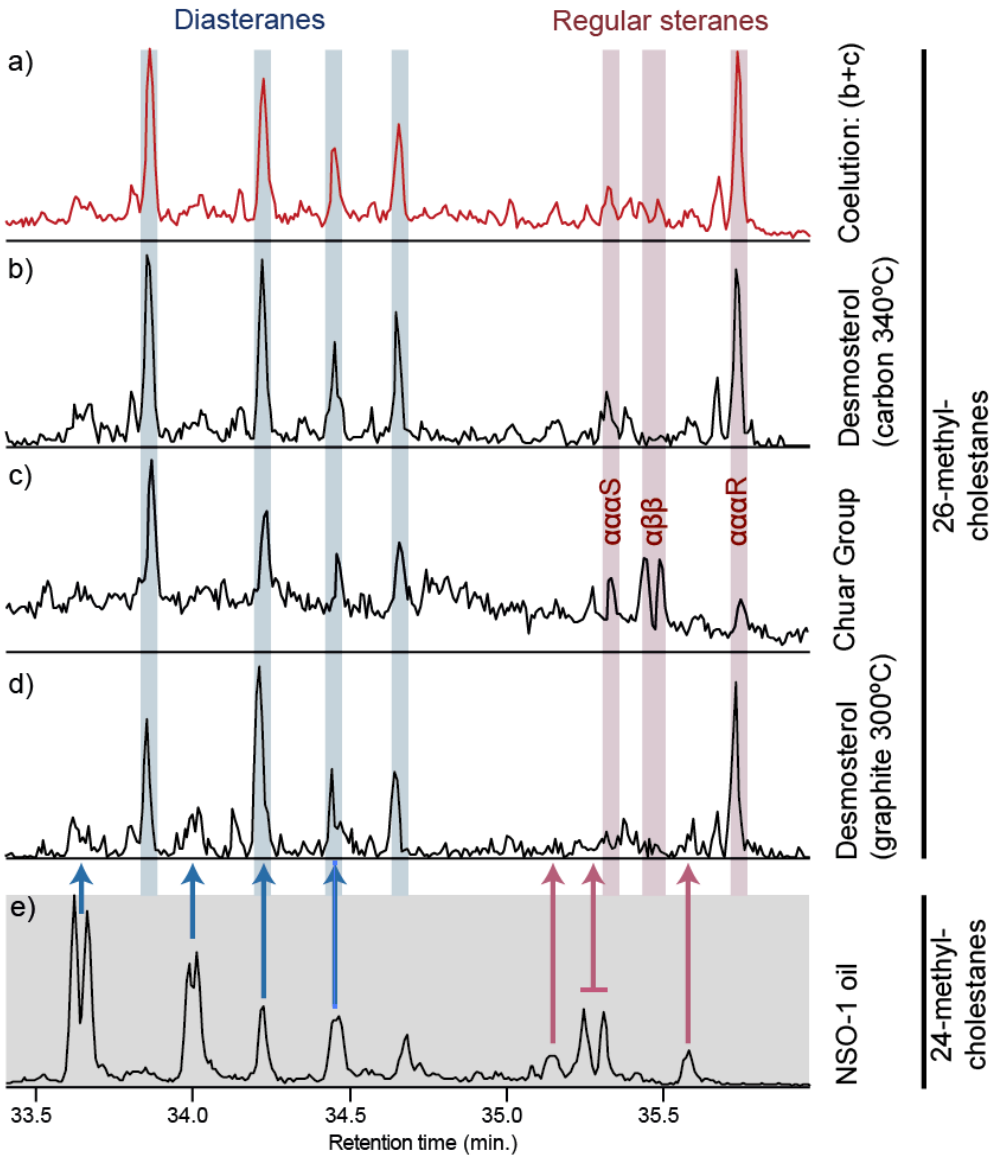

Supplementary Figure 1. Comparison between 26-methylcholestanes in Neoproterozoic rocks and in laboratory pyrolysates. Chromatograms **(***m/z* 386→217) showing 26-methylcholestanes in a) a co-injection-experiment of desmosterol pyrolysate (b) and Chuar Group bitumen (c), b) an active carbon-based desmosterol pyrolysate (340ºC, #5 in Supplementary Table 1), c) a Chuar Group extract (sample #L.38 in reference[5]), and d) a graphite-based desmosterol pyrolysate (300ºC, #8 in Supplementary Table 1). The elution pattern of 26-methylcholestanes (a–d) is distinct from that of common C_{28} steranes (24-methylcholestanes) found in most Phanerozoic rocks and oils, as exemplified by e) Phanerozoic oil NSO-1 reference standard[6]. Note that in contrast to regular steranes, 24*S* and *R* isomers of rearranged 24-methylcholestanes (diaergostanes) can be partly separated under common chromatographic conditions; therefore diaergostane peaks in (e) are split. The co-injection experiment illustrates that not only the ααα*R* regular cryostane (26-mec) isomer, but also the four main diasterane (re-arranged) isomers formed during pyrolysis. As typical for matured geological samples, the Chuar Group sample (c) additionally contains the ααα*S* and αββ *R* and *S* geological rearranged isomers that are low or absent in the pyrolysates.

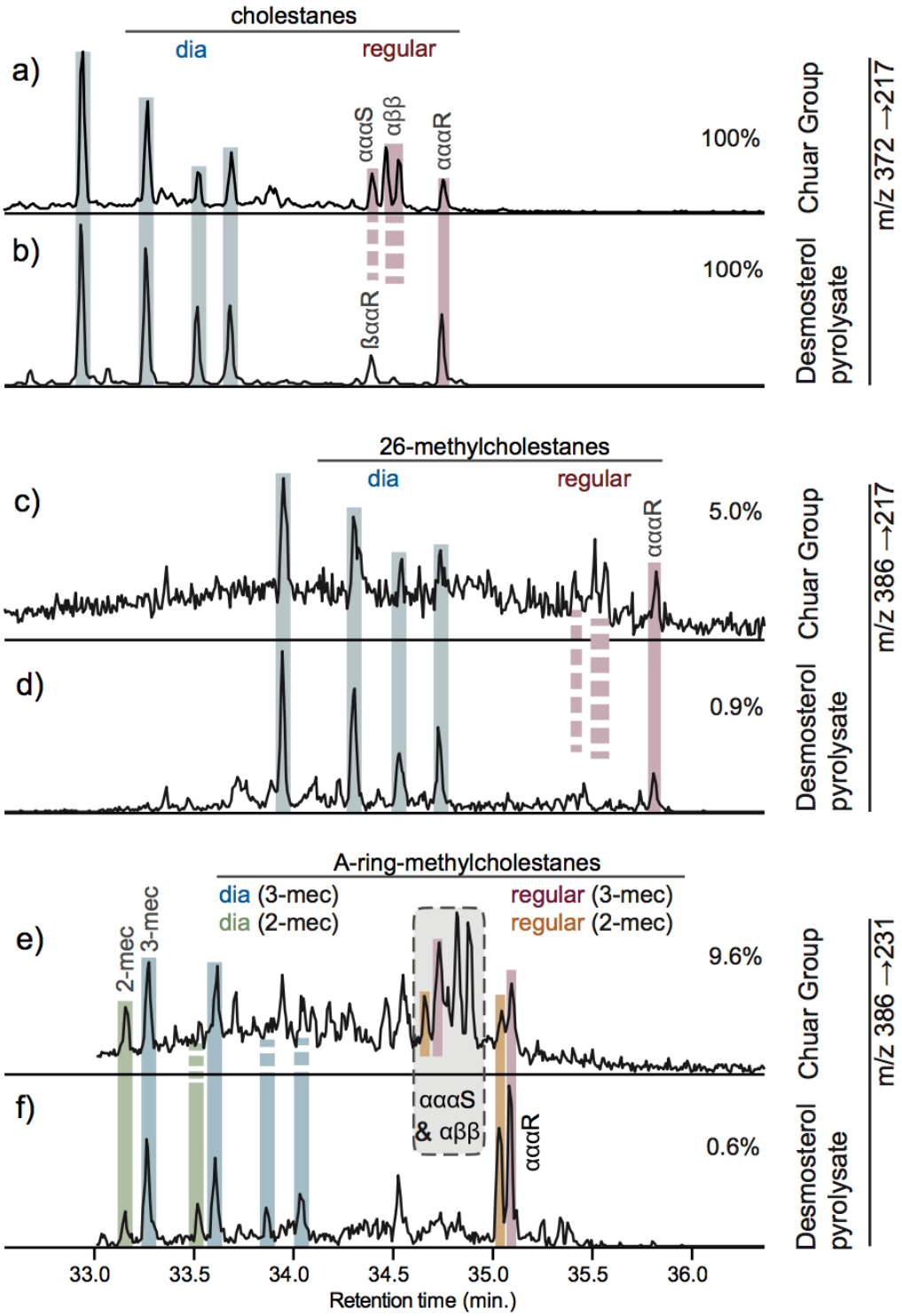

Supplementary Figure 2. Comparison of C_{27} (a, b) and C_{28} (c–f) sterane signatures in Chuar Group rock extract L.38 (a, c, e) and desmosterol pyrolysate (b, d, f; 340ºC on active carbon, #6 in Supplementary Table 1). The comparison shows that Tonian-like signatures are produced in the carbon-surface-assisted pyrolysis of desmosterol. The similarities include the dominance of regular and re-arranged (diasteranes) isomers of cholestane in addition to lower relative concentrations of 2-, 3- and 26-methylcholestanes and roughly similar relative abundances of dia- and regular steranes, and of cholestanes relative to the different methylated cholestanes. Key: 3-mec, 3-methylcholestane, 2-mec, 2-methylcholestane. At right, percent values represent a measure of signal intensity relative to the C_{27} steranes in each sample (note that reported abundances were determined from individual peak areas).

The elution pattern-based inference that the C_{28} alkylsteranes produced during pyrolysis correspond to those found in Neoproterozoic rock extracts was confirmed by co-injecting pyrolysates with rock extracts from the Tonian Chuar Group (Supplementary Figure 1a). Additionally, the identity of the pyrolytic ααα*R* 26-mec isomer was confirmed by co-injection with an authentic 26-mec standard[7] (Supplementary Figure 3). Comparing the retention time of tentatively identified ααα*R* isomers of higher homologs of the 26-alkylated series in Tonian rock extracts to peaks in our pyrolysates, we were able to trace the 26-alkylsterane series in pyrolysates at least to the three-carbon substituted C_{30} sterane tentatively identified as 26-*n*-propylcholestane (26-proc; also see the discussion about identifying 26-proc in Zumberge et al., 2019[2], and in the Supplementary Information of Brocks et al., 2017[8]). Higher homologs (particularly C_4 and C_5 alkylated) are also present, but structural identification becomes more difficult (see Figure 2e).

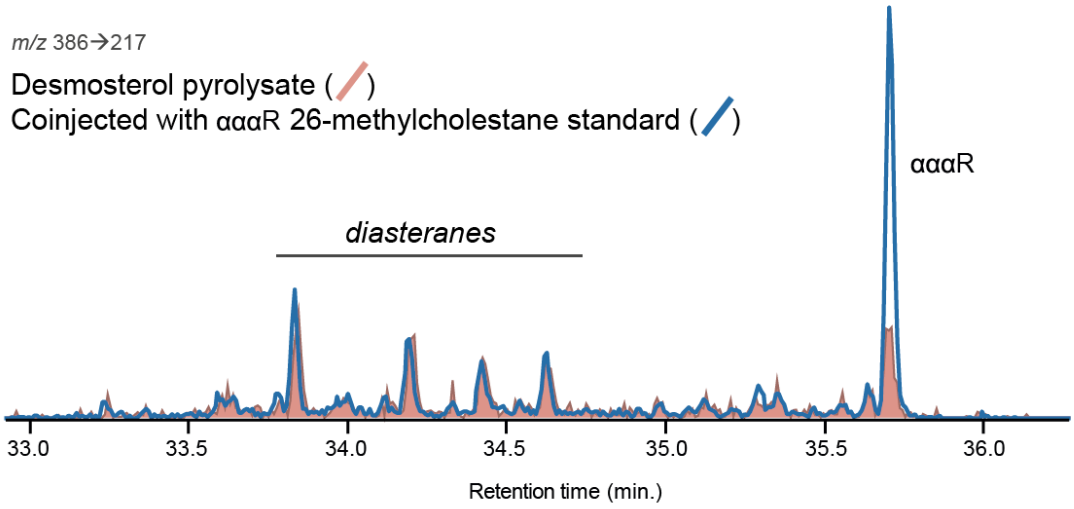

Supplementary Figure 3. GC-MS co-injection experiment of a desmosterol pyrolysate and an authentic standard of ααα*R* 26-mec (cryostane). Chromatogram (*m/z* 386→217 transition) showing a desmosterol graphite pyrolysate (340ºC for 24 h; #4 in Supplementary Table 1), and co-injection with a 26-mec standard synthesised by P. Adam and P. Schaeffer[7].

In pyrolysates, as well as in rock extracts of the Chuar and Araras Groups, we also observed an alkylated series, similar to the 26-alkylated series, for position C-3 of the steranes. For low molecular weight homologs (C_1–C_3 alkylation), pyrolysate products match those found in Neoproterozoic sediments (Supplementary Figure 2e,f for C_1-alkylated steranes) and represent a continuous linear alkyl extension. However, the main peaks representing higher molecular weight 3-alkylsteranes (substituted with four or more carbon units) in the pyrolysates elute earlier than the *n*-alkyl homologs that are found in many rock extracts and oils[9–11] and which were previously identified in Neoproterozoic Araras Group extracts by coelution experiments with synthetic standards[9]. Thus while $C_{1\text{-}3}$ alkylations represent methyl, ethyl and *n*-propyl-steranes, the main higher alkylated homologs of pyrolysates do not represent linear chain extensions. Based on their early elution positions[10], they likely represent 3-isoalkylsteranes that have previously been identified in a large variety of geological samples (including Cambrian rock extracts from the Alum Shale and Inca Formation), and can be more abundant than their *n*-alkyl homologs[10]. Previous laboratory experiments with radical initiators

have demonstrated that when alkylation proceeds *via* radical chain reactions, large alkyl homologs of up to eight carbon atoms can readily be fused with other hydrocarbons[12].

For higher molecular masses in the pyrolysates, the selected ion chromatograms of the M^+→ *m/z* 217 series, which are typically dominated by regular (desmethyl) and side-chain-alkylated steranes, show additional prominent peaks. Some of these peaks likely represent 3-alkylsteranes as they are also visible in M^+→ (217+x*14) chromatograms but with notably higher intensities (x representing the number of carbon atoms attached to C-3). MRM chromatograms of our authentic 3-*n*-propylcholestane standard confirmed that the elution of 3-alkylsteranes also results in the appearance of respective peaks in M^+→ *m/z* 217 chromatograms. As implied in the basic reaction scheme in Fig. 1f, 26- and 3-alkylsteranes may form simultaneously.

2) Pyrolytic formation of 26-mes from C_{29} sterols

Many rock extracts and oils of Ediacaran to Cambrian age contain elevated relative abundances of the C_{30} sterane 26-methylstigmastane (26-mes), which was recently proposed to represent another sponge-diagnostic biomarker[13]. To test if side-chain functionalised C_{29} sterols may also become alkylated at position 26 in laboratory maturation experiments, we subjected different side-chain functionalised C_{29} sterols (stigmasterol, clerosterol, fucosterol) to the same type of pyrolysis experiments that had resulted in the formation of 26-mec from side-chain functionalised C_{27} sterols.

Similar to the C_{28} 26-alkylsterane distributions in *m/z* 386→217 chromatograms (Supplementary Figure 1b,d) arising from the pyrolysis of C_{27} sterols, the *m/z* 414→217 chromatograms (i.e. corresponding to C_{30} steranes) of C_{29} stigmasterol pyrolysates are characterised by five very late eluting C_{30} sterane isomers comprising four diasteranes and the ααα*R* isomer (Supplementary Figure 4a). The strong *m/z* 217 fragment indicates methylation at the side-chain—not in the ring system—whereas the late elution position points towards terminal methylation[13]. In analogy to pyrolytic 26-methylcholestane (C_{28} 26-mec) formation from desmosterol, it would thus appear that 26-methylstigmastane (C_{30} 26-mes) is the main C_{30} sterane formed in our stigmasterol pyrolysis experiment.

The identity of the ααα*R* isomer of 26-mes was confirmed by co-injection experiments with Ediacaran rock extracts (Supplementary Figure 5), and with a sponge hydropyrolysate of *R. distincta* (Supplementary Figure 4) kindly provided by G. Love (UC Riverside), which was used for the original identification of 26-mes in ancient rocks[13]. The sponge HyPy extract also appeared to contain trace concentrations of the 26-mes diasterane re-arrangement products (inset in Supplementary Figure 4; cf. Supplementary Figure 4 in[13]). These small peaks in the *R. distincta* hydropyrolysate chromatogram elute in the same positions as the main peaks in the *m/z* 414→217 trace of the stigmasterol pyrolysate (Supplementary Figure 4a), supporting the identification of 26-mes diasteranes in the stigmasterol pyrolysate. Our pyrolysis experiments thus suggest that 26-methylstigmastanes can form through abiogenic geological alteration of regular side-chain functionalised sterols such as stigmasterol. Accordingly, biogenic C_{30} sterol precursors are not needed to explain the occurrence of C_{30} steranes in Ediacaran and Cambrian aged rock extracts and oils (see also Bobrovskiy et al., this issue[14]).

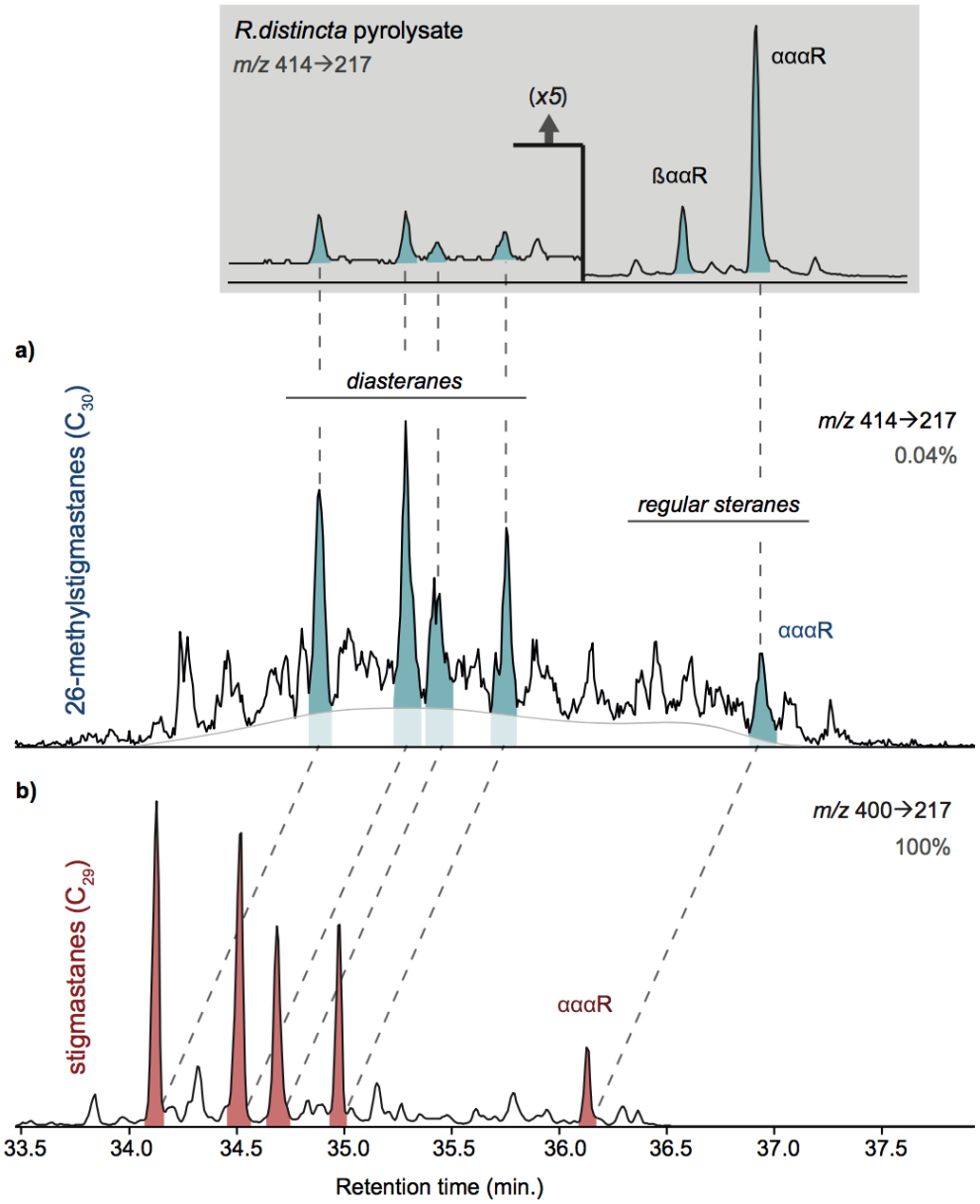

Supplementary Figure 4. Comparison of elution patterns of C_{29} stigmastanes and C_{30} steranes in a stigmasterol pyrolysate. a) Chromatogram (*m/z* 414→217) highlighting the inferred isomers of C_{30} 26-mes. Note that the identity of the ααα*R* 26-mes peak was confirmed by co-elution experiments using rock extracts (Supplementary Figure 5) and a sponge pyrolysate (grey shaded box and Supplementary Figure 5; *Rhabdastrella distincta* sample provided by Prof. Gordon Love). b) Chromatogram (*m/z* 400→217) highlighting five main isomers of stigmastane, comprising four diastigmastanes and ααα*R* stigmastane (#19 in Supplementary Table 4). At right, percent values represent a measure of signal intensity relative to the C_{29} steranes (note that reported abundances were determined from individual peak areas).

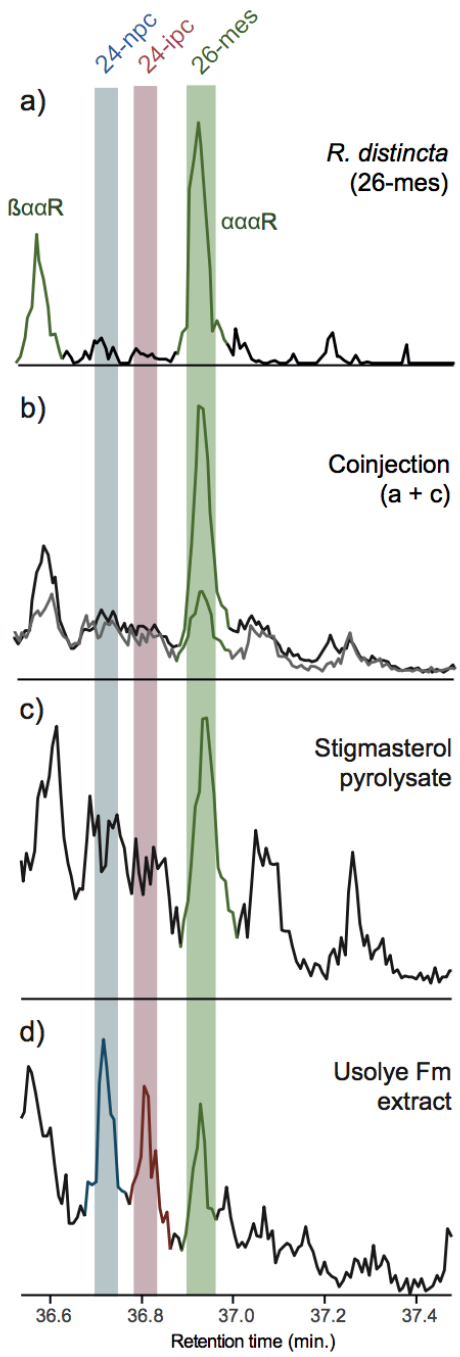

Supplementary Figure 5. Elution range of αααR 26-mes in a sponge HyPy extract, rock extract and stigmasterol pyrolysate in *m/z* 414→217 GC-MS chromatograms. Identity of the αααR 26-mes isomer in a) hydropyrolysate of the sponge *Rhabdastrella distincta* was determined by Zumberge et al.[13] (sample provided by Prof. G. Love). b) A coelution experiment (upper trace) of a stigmasterol pyrolysate (lower trace in b, and c) with the *R. distincta* pyrolysate (a) confirms the pyrolytic formation of 26-mes. c) The stigmasterol pyrolysate (#19 in Supplementary Table 4) used in the co-elution experiment. The identity of 26-mes was additionally corroborated by coelution experiments with d) extracts of the Usolye Formation, which contains all three putative sponge steranes[15].

3) Abundances of methylsteranes in Neoproterozoic rocks and pyrolysates

3.1 26-methylcholestane abundances

Although our pyrolysis experiments can only simulate part of the diagenetic processes that may result in elevated abundances of alkylated steroids in natural environments, we observed notable alkylation yields of up to 2.0% at the C-26 position (Supplementary Table 1). The proportion of 26-methylcholestane relative to cholestane obtained in our C_{27} sterol pyrolysates is thus comparable to that encountered in Neoproterozoic rock extracts (2–8% relative to cholestane, average 4.8%, *n* = 10 reported by Zumberge et al., 2019, for rock extracts and pyrolysates from the Chuar and Visingsö Group[2]; 3.0–7.7% in our analyses of rock extracts from the Chuar and Araras groups, average 4.9% relative to cholestane [*n* = 13, Supplementary Table 2]). This similarity suggests that abiogenic diagenetic alteration of regular side-chain functionalised C_{27} sterol precursors can account for the abundance of 26-mec in Neoproterozoic sedimentary rocks.

While laboratory-controlled pyrolysis experiments generally simulate geological maturation processes of organic matter quite well, a difference in yields is noticeable. The observed range in alkylation yields between different pyrolysis experiments (<<0.1 to 2.5%; Supplementary Table 1) suggests that small differences in experimental conditions can influence the alkylation yields. In our experiments, alkylation took place in both untreated and siloxane-deactivated glass tubes, indicating that glass surfaces do not play a significant role in the alkylation processes. If anything, deactivation may increase alkylation yield (see Supplementary Table 1). While we have not yet identified which factors influence alkylation yields in experiments with the same sterol precursors, our data clearly show that alkylation yields are higher for sterols with additional functional groups (desmosterol, 25-hydroxycholesterol: average 3-methylsterane yields of 1.85% relative to cholestane, *n* = 10) compared to cholestanol with only a single functional group (average 0.13%, *n* = 4; Supplementary Table 1). While the presence of a double bond at C-5 is likely to enhance the reactivity of the C-3 position, the observation that alkylation yields are similar for alkylation at C-3 and C-26 in desmosterol experiments (Supplementary Table 3) suggests that, when other reactive compounds are lacking, alkyl donation through side-chain decomposition (in turn favoured by the presence of functional groups in the side-chain) is a major factor for the alkylation of sterols under our pyrolytic conditions. In view of previously inferred differences for the extent of methylation and radical reactions during petroleum formation, the relatively large range in pyrolytic alkylation yields suggests that in natural environments under particular diagenetic conditions, certain factors such as the presence of radical initiators[12,16] and/or effective alkyl donors might significantly increase alkylation yields as previously inferred for sulphide-induced radical-chain reactions as a control on petroleum formation rates in source rocks[16] and intermolecular methyl-transfer from poly-methylated polyaromatic hydrocarbons in natural samples[17,18].

Supplementary Table 1. Experimental conditions, 26-mec and 3-mec yields (as % of cholestane, ααR isomers only) for different C_{27} sterol in the pyrolysis experiments.

#	Sterol	Other	Solid phase	T (°C)	Time (h)	Silanized	26-mec (% cholestane)	3-mec (% cholestane)
1	25-hydroxycholesterol	*n*-C_{15}	graphite	310	24	no	1.1	2.5
2	25-hydroxycholesterol		graphite	300	24	no	0.3	1.5
3	25-hydroxycholesterol	clerosterol	graphite	300	24	no	1.8	2
4	desmosterol		graphite	340	24	yes	1.5	2.5
5	desmosterol		AC	340	24	no	0.8	2
6	desmosterol		AC	340	24	no	0.5	1.5
7	desmosterol		AC	300	24	no	1	1.8
8	desmosterol		graphite	300	24	no	1	2.1
9	desmosterol		graphite	300	24	yes	0.3	1.9
10	desmosterol		AC	300	24	yes	2	0.8
11	cholesterol	*n*-C_6	graphite	300	24	no	<< 0.1	0.8
12	cholestanol		graphite	340	24	no	0	0.1
13	cholestanol		AC	340	24	yes	0	0.1
14	cholestanol		AC	310	24	no	<< 0.1	0.2
15	cholestanol		AC	300	24	yes	0	0.2
16	cholest-2-ene		AC	300	24	yes	<< 0.1	0.1

Key: AC, activated carbon; T., pyrolysis temperature; 26-mec, 26-methylcholestane; 3-mec, 3-methylcholestane; n-C_{15}, n-pentadecane addition; n-C_6, n-hexane addition.

Supplementary Table 2. Comparison of 26-mec (ααR) and 3-mec (ααR) yields as percentage of cholestane (ααR) observed in the Neoproterozoic Araras and Chuar Group.

#	26-mec (% cholestane)	3-mec (% cholestane)	3-mec / 26- mec	Formation / Member	Group
Te.S 22	3.45	22.46	6.51	Mirassol d'Oeste Fm.	Araras Group
Te.S 30	3.14	20.11	6.40	Guia Fm.	Araras Group
LvM-00347	4.72	18.30	3.88	Mirassol d'Oeste Fm.	Araras Group
LvM-00350	4.21	18.34	4.36	Mirassol d'Oeste Fm.	Araras Group
L.30	5.50	9.34	1.70	Walcott Member	Chuar Group
L.31	6.43	14.06	2.19	Walcott Member	Chuar Group
L.32	4.76	14.22	2.99	Walcott Member	Chuar Group
L.33	2.98	13.59	4.56	Walcott Member	Chuar Group
L.34	3.08	10.41	3.38	Walcott Member	Chuar Group
L.39	7.65	13.67	1.79	Walcott Member	Chuar Group
L.46	6.97	12.35	1.77	Walcott Member	Chuar Group
L.47	5.55	16.55	2.98	Walcott Member	Chuar Group
L.48	5.99	12.56	2.10	Walcott Member	Chuar Group

3.2 Calculating pyrolytic alkylsterane yields

Due to common coelution of diasteranes with other compounds, the late eluting ααR sterane isomer is usually the best resolved chromatographic peak in geological samples. Therefore, methylcholestane/cholestane ratios in Supplementary Tables 1 and 2 are restricted to the ααR isomer. To test for potential differences in calculated alkylsterane/desmethylsterane

ratios when only ααR isomers are considered—*versus* when all main isomers are considered—in Supplementary Table 3 we also calculated 26-mec and 3-mec yields as percentage of cholestane when diasteranes are included (ααR and ααS/βαR, and the four main diasterane peaks shown in Supplementary Figure 2a, d, f). As we observed low 3-methyldiasterane yields in most pyrolysates, we restricted the comparison to a limited number of pyrolysates for which we were able to confidently identify all four 3-mec diasterane peaks (Supplementary Figure 2f that exhibits a sample with some of the highest observed 3-methyldiasterane yields).

Since 26-mec shows similar diasterane distributions as cholestane in the same experiments (cf. Supplementary Figure 2b vs 2d), 26-mec yields (expressed as % of cholestane) are very similar for either ααR-only or diasterane-inclusive calculations. In contrast, due to the low relative diasterane yields for 3-mec in most pyrolysis experiments, 3-mec yields are significantly higher if only the ααR is considered. In diasterane-inclusive calculations, 3-mec yields are broadly comparable, yet slightly lower, compared to 26-mec yields (Supplementary Table 3). The slightly lower 3-mec yields can be explained through the formation of other A-ring methylated sterane isomers (dominantly 2-methyl), which in most pyrolysates (Supplementary Figure 2f) and geological samples[11] occur in lower concentrations than the 3-methyl isomers.

Supplementary Table 3. Comparison of 26-mec and 3-mec yields as percentage of cholestane when calculated for ααR isomers only or when ααS and the four main diasterane peaks are included in calculations. Experiments are the same as in Supplementary Table 1. The diasterane isomers included in the calculations are marked with filled circles in Supplementary Figure 2.

#	Precursor sterol	26-mec		3-mec	
		(% cholestanes) Incl. diasteranes	(% cholestane) Only ααR	(% cholestanes) Incl. diasteranes	(% cholestane) Only ααR
2	25-hydroxycholesterol	0.4	0.3	0.3	1.5
4	desmosterol	1.9	1.5	1.3	2.5
6	desmosterol	0.8	0.5	0.6	1.5
7	desmosterol	0.9	1	0.6	1.8
8	desmosterol	1	1	0.6	2.1
9	desmosterol	0.4	0.3	0.4	1.9
15	cholestanol	0	0	0.1	0.2

3.3 Abundance of 26-mes in Neoproterozoic rocks and pyrolysates

Pyrolysis yields of 26-mes in abundances comparable to those found in Ediacaran and Cambrian aged rock extracts suggest that abiogenic geological alteration of regular C_{29} sterols may account for the geological occurrence of 26-mes. As with 26-mes normalised to cholestane to gauge the degree of alkylation of C_{27} sterol precursors, we consider the normalisation of 26-mes to C_{29} stigmastane suitable for the comparison between potential alkylation yields in pyrolysates *versus* rock samples. Since 26-mes concentrations or the abundance of 26-mes relative to C_{29} steranes have not yet been reported in the literature, we calculated 26-mes as percentage of stigmastane for Neoproterozoic and Cambrian bitumens and HyPy products from the data reported in Supplementary Tables 1 and 2 of Zumberge et al. (2018)[13] (%C_{29} and %C_{30} steranes, 24-ipc ppm sats, 26-mes ppm sats, 24-ipc/24-npc and 26-mes/24-ipc ratios) as 0.3–4.2%, average 1.5%, n = 61.

In our pyrolysis experiments with pure sterols, the proportion of pyrolytic 26-mes relative to C_{29} stigmastane (0.1–0.8%, average 0.4% Supplementary Table 4) overlaps with those typically encountered in Neoproterozoic-Cambrian rock samples. Thus, just as for 26-mec, the pyrolysis experiments suggest that abiogenic geological alkylation may account for 26-mes in ancient rocks.

Supplementary Table 4. Experimental conditions and 26-mes yields (as % of C_{29} stigmastane; calculated for ααR isomers) obtained during the pyrolysis of different C_{29} sterols. All experiments were carried out in non-deactivated tubes at 300ºC for 24 h, except for #17, which was run for 38 h at 300ºC employing a deactivated glass tube.

#	sterol	other	solid phase	26-mes (% stigmastane)
17	fucosterol		graphite	0.8
18	fucosterol	*n*-hexane	graphite	0.4
19	stigmasterol	*n*-hexane	graphite	0.1
20	clerosterol		activated carbon	0.3
3	clerosterol	25-hydroxycholesterol	graphite	0.3

4) Alkylation mechanisms and product distribution

While a detailed understanding of the precise mechanisms of the observed alkylation reactions is beyond the scope of this study and not required to recognise diagenetic alkylation products in the rock record, we consider radical and/or cationic reactions, mediated by solid carbon surfaces[19], as most plausible. In our pyrolysis experiments, the thermal cracking of hydrocarbons in the presence of solid carbon surfaces is thought to trigger the formation of reactive alkyl moieties of different chain lengths (up to C_8) deriving from cracking of the steroid side-chain. This is corroborated by abundance minima of C_2 and C_7 alkylsteranes (not shown), corresponding to the isoprenoidal branching points in the steroid side-chain of the educt. Radical reactions are likely to result in the formation of radical and unsaturated alkyl moieties, whereas acidic sites may also produce cationic alkyl intermediates[20]. The reactive alkyl moieties generated by the carbon-catalysed cracking of the steroid side-chains are then available for alkylation of other steroids. Both radical and cationic processes can be envisaged to play a role in the alkyl transfer reactions occurring in both pyrolysates and geological environments[17,19,21] and to account for the generation of new C-C bonds involved in the formation of 3- and 26-alkylsteranes.

In our pyrolysis experiments, where decomposing sterol molecules are probably the dominant alkyl donors, thermochemical cracking of the sterol side-chain is likely to be the source of alkyl moieties. Therefore, relatively large alkyl moieties (up to C_8) may be transferred, a process that could explain relatively high concentrations of higher (> C_2-alkylated) homologs (cf. Fig. 2e). In geological transformations of natural organic matter, the intermolecular transfer of reactive methyl groups from a variety of chemical compounds is thought to provide a reactive 'methyl pool' that can be accessed by every molecule in a sedimentary bitumen and crude oil[18]. Accordingly, depending on the exact composition of the organic material and the specific diagenetic conditions, a large variety of potentially reactive alkyl moieties can be produced.

Despite wide differences in geographic location (Amazonia [present day Brazil] *versus* Laurentia [present day USA]) and time of deposition (~740 *versus* 635 Ma), the Chuar and Araras Group extracts yield intriguingly similar homolog distribution patterns for both 3- and

26-alkylcholestanes (Fig. 2a–c). In both settings, the relative distribution of higher alkylated homologs can be described by an exponential decrease (Fig. 2a, b). This distribution is evocative of the sequential addition of methyl groups, but it also presents some analogies with the commonly observed exponential decrease of *n*-alkanes with increasing carbon number in rock extracts and oils of elevated maturity. The distribution could thus reflect extended *n*-alkyl moieties that were added earlier in the burial history of the sedimentary rocks *via* diagenetic processes and that were subsequently cracked by geothermal processes in a similar manner to *n*-alkanes and other hydrocarbon chains. The distribution of the alkylated sterane homologues in geological samples and pyrolysates could thus be controlled both by the nature and size of the reactive alkyl moieties available for alkylation and by the progressive thermal degradation of alkyl moieties.

5) Potential to differentiate biogenic from abiogenic origins of biomarkers

The observation that supposedly biologically-diagnostic hydrocarbon skeletons of specific biomarkers, such as steranes, can be generated by geological alkylation may have far-reaching implications for paleo-ecological interpretations and needs to be taken into consideration in biomarker interpretations. However, the observation will not generally challenge the biomarker concept as organic geochemists have long been aware that diagenetic and catagenic processes affect the relative abundances and structures of biomarkers. In the same way that biomarker proxies were developed to gauge the degree of thermal alteration, it may be possible to develop proxies—such as the (2-methyl + 3-methylsterane)/desmethylsterane ratio—to gauge the degree of diagenetic alkylation and use this information to interpret other minor steranes. However, biogenic *versus* abiogenic sources of minor alkylated steranes are unlikely to be resolved by relative compound abundances alone. Rather, we need to look for distribution patterns such as the occurrence of extended alkylated series, or for correlations between ambiguous steranes (e.g. 26-alkylsteranes) and clearly diagenetic steranes (e.g. 3-alkylsteranes). We are confident that organic geochemists will uncover criteria to differentiate between biogenic and abiogenic origins of such biomarkers.

Supplementary References

1. Rooney, A. D. *et al.* Re-Os geochronology and coupled Os-Sr isotope constraints on the Sturtian Snowball Earth. *Proc. Natl. Acad. Sci. U. S. A.* **111**, 51–6 (2014).

2. Zumberge, J. A., Rocher, D. & Love, G. D. Free and kerogen-bound biomarkers from late Tonian sedimentary rocks record abundant eukaryotes in mid-Neoproterozoic marine communities. *Geobiology* **18**, 326–347 (2020).

3. van Maldegem, L. M. *Molecular and isotopic signatures of life surrounding the Neoproterozoic Snowball Earth events*. *PhD Dissertation, University of Bremen* (https://media.suub.uni-bremen.de/handle/elib/1535, 2017).

4. Seifert, W. K. & Moldowan, J. M. Applications of steranes, terpanes and monoaromatics to the maturation, migration and source of crude oils. *Geochim. Cosmochim. Acta* **42**, 77–95 (1978).

5. van Maldegem, L. M. *et al.* Bisnorgammacerane traces predatory pressure and the persistent rise of algal ecosystems after Snowball Earth. *Nat. Commun.* **10**, 1–11 (2019).

6. Weiss, H. The Norwegian industry guide to organic geochemical analyses. *Ed. 4.0 Nor. Hydro Statoil, Geolab Nor. SINTEF Pet. Res. Nor. Pet. Dir.* (2006).

7. Adam, P., Schaeffer, P. & Brocks, J. J. Synthesis of 26-methyl cholestane and identification of cryostanes in mid-Neoproterozoic sediments. *Org. Geochem.* **115**, 246–249 (2018).

8. Brocks, J. J. *et al.* The rise of algae in Cryogenian oceans and the emergence of animals. *Nature* **548**, 578–581 (2017).

9. Sousa Júnior, G. R. *et al.* Organic matter in the Neoproterozoic cap carbonate from the Amazonian Craton, Brazil. *J. South Am. Earth Sci.* **72**, 7–24 (2016).

10. Dahl, J. E. *et al.* Extended 3β-alkyl steranes and 3-alkyl triaromatic steroids in crude oils and rock extracts. *Geochim. Cosmochim. Acta* **59**, 3717–3729 (1995).

11. Summons, R. E. & Capon, R. J. Identification and significance of 3β-ethyl steranes in sediments and petroleum. *Geochim. Cosmochim. Acta* **55**, 2391–2395 (1991).

12. Urry, W. H., Stacey, F. W., Huyser, E. S. & Juveland, O. O. The Peroxide- and Light-induced Additions of Alcohols to Olefins. *J. Am. Chem. Soc.* **76**, 450–455 (1954).

13. Zumberge, J. A. *et al.* Demosponge steroid biomarker 26-methylstigmastane provides evidence for Neoproterozoic animals. *Nat. Ecol. Evol.* **2**, 1709–1714 (2018).

14. Bobrovskiy, I. *et al.* Algal origin of sponge sterane biomarkers negates the oldest evidence for animals in the rock record. *Nat. Ecol. Evol.* This Issue

15. Nettersheim, B. J. *et al.* Putative sponge biomarkers in unicellular Rhizaria question an early rise of animals. *Nat. Ecol. Evol.* **3**, 577–581 (2019).

16. Lewan, M. D. Sulphur-radical control on petroleum formation rates. *Nature* **391**, 164–166 (1998).

17. Alexander, R., Bastow, T. P., Fisher, S. J. & Kagi, R. I. Geosynthesis of organic compounds: II. Methylation of phenanthrene and alkylphenanthrenes. *Geochim. Cosmochim. Acta* **59**, 4259–4266 (1995).

18. Bastow, T. P. *et al.* Geosynthesis of organic compounds. Part V - Methylation of

alkylnaphthalenes. *Org. Geochem.* **31**, 523–534 (2000).

19. Alexander, R., Berwick, L. & Pierce, K. Single carbon surface reactions of 1-octadecene and 2,3,6-trimethylphenol on activated carbon: Implications for methane formation in sediments. *Org. Geochem.* **42**, 540–547 (2011).

20. Greensfelder, B. S., Voge, H. H. & Good, G. M. Catalytic and Thermal Cracking of Pure Hydrocarbons: Mechanisms of Reaction. *Ind. Eng. Chem.* **41**, 2573–2584 (1949).

21. Given, P. H. & Hill, L. W. Catalysis of the isomerisation and polymerisation of olefins on carbon blacks. *Carbon* **6**, 525–535 (1968).